Designing a Boosting Microthruster for Altitude Maintenance of Picosatellites

Rishvinder Singh, Mohamed Faiz bin Mohamed Abdul Kadir
Nanyang Technological University
50 Nanyang Avenue, Block N3, Singapore 639798
RISH0009@e.ntu.edu.sg, FAIZ003@e.ntu.edu.sg

Faculty Advisor: Asst Prof Li King Ho, Holden
Nanyang Technological University

ABSTRACT

More countries are relying on small satellites to conduct research in Low-Earth Orbit (LEO). This has increased focus on developing microthrusters to counter atmospheric drag. This paper aims to design such a microthruster for the CubeSat to augment orbital lifetime and allow more meaningful space experimentation. This was done by first selecting an available microthruster design that met altitude boosting requirements. This design was then reconstructed with material changes, and tested for material suitability. A second design, with optimised geometry, was then conceptualised. This new microthruster will use 3,3(')-azobis(6-amino-1,2,4,5-tetrazine)-mixed N-oxides (DAATO3.5) as its solid propellant. However, due to import restrictions, tests were performed using ammonium carbonate and comparisons were made to approximate the performance of DAATO3.5, by calculating an efficiency factor (η) based on simulated and experimental results. Prototypes with ammonium carbonate were tested in vacuum (10-3 mbar) and gave a specific impulse of 9.15 s. This was found to be 22.21% (η) of simulated results. Applying this factor to DAATO3.5 gave a specific impulse of 24.9 s for a 16-microthruster array. This would give an altitude gain of 5.45 km, increasing orbital lifetime by 20% (12 days).

INTRODUCTION

1.1 Project Background

In 1999, California Polytechnic State University and Stanford University jointly developed the CubeSat, to help university students access space[1]. Each unit of these picosatellites was a cube with 10 cm length, weighing at most 1.33 kg [2,3].

They are typically launched in Low-Earth Orbit (LEO), between altitudes of 160 km and 1000 km, for testing and data collection missions[4]. CubeSats can be deployed either as a single unit (1u), or stacked in a group of a maximum of 16 units (16u)[5]. Since the first CubeSat launch, there has been immense growth in the number of successful launches, as seen in Figure 1.

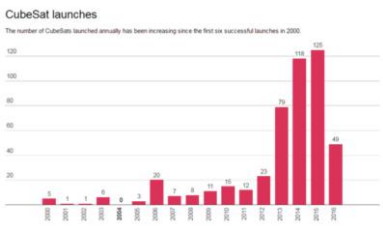

Figure 1: Number of CubeSat Launches by Year[6]

The explosive growth in the popularity of CubeSats is partly due to the low cost of launch, estimated to be around US$40,000. Launching a conventional satellite can cost millions of dollars[2]. This has given a strong enough impetus for developing nations, like Pakistan, Estonia and Colombia, to venture into space exploration, with CubeSats as their first satellites[6].

1.2 Project Motivations & Aim

In LEO, CubeSats are still subjected to atmospheric drag, which will slow them down, causing them to deorbit sooner. While CubeSats can level the playing field across nations in terms of space exploration, their orbital lifetimes are still a limiting factor. Estimates of the lifetimes of a 1u CubeSat are shown in Table 1.

Table 1: Initial Orbital Altitude against Orbital Lifetime for 1u CubeSat[7]

Initial Orbital Altitude (km)	Orbital Lifetime
300	18 days
350	58 days
400	167 days
450	1.1 years
500	2.4 years

This hinders the ability of developing nations to catch up with countries with established space agencies, such as the United States and Russia. For developing countries, more time in space would enable more extensive research to be conducted, which may help in the areas of space readiness testing, scientific advancement, and the development of commercial opportunities, such as those in agriculture and city planning[5]. Hence, there is a strong motivation to prolong orbital lifetime, since this can, in the long run, pave the way for economic growth, national development and technological advancements. Such advancements would allow developing nations to cut off their dependence on first-world countries.

Hence, the aim of this project is to design and test a CubeSat microthruster that can produce enough thrust to boost it to a higher altitude and extend its lifetime.

1.3 Approach Taken

This project begins with the selection of a currently available microthruster. This will be adapted, by making changes to its dimensions and materials, before being assembled and subsequently put through experiments to determine the materials' suitability. Using these findings, a second, improved design will be assembled and tested, to determine if its performance is satisfactory.

MICROTHRUSTER SELECTION

Ion, cold gas and solid propellant microthrusters were considered for this project. Table 2 compares these different microthrusters.

Table 2: Table of Comparison for Different Microthrusters[8 9 10 11 12 13]

Parameters	Ion	Cold Gas	Solid Propellant
Volume	High	High	Low
Mass	Low	High	Low
Required Power	High	Low	Low
Thrust	Low	High	High
Repeated Use	Yes	Yes	No

Table 2 shows that solid propellant microthrusters have optimal performance in the top 4 categories. Its main downside, of being single-use, is not disadvantageous if its application is simply an altitude boost. Hence, a solid propellant microthruster was chosen.

2.1 Microthruster Design to be Adapted

The exact solid propellant design that was adapted was that of Chaalane et al.[14,15]. Their MicroElectroMechanical Systems (MEMS)-based microthruster was manufactured using Deep Reactive-Ion Etching (DRIE), and comprises of a silicon layer sandwiched between a layer of Pyrex glass and one of Macor ceramic. This is illustrated in Figure 2 below.

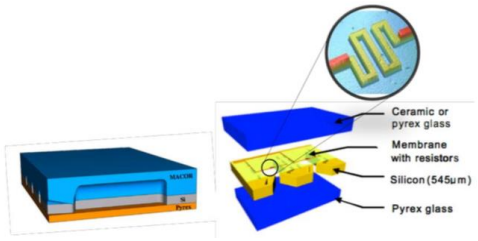

Figure 2: Illustration of Microthruster Layers

The silicon layer includes the 20 mm^3 propellant chamber and nozzle. A thin SiO_2/SiN_X membrane sits above this layer and holds the igniters. Figure 3 shows a top-down view of the silicon layer.

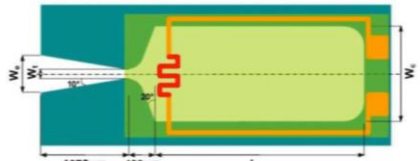

	Wc	We	Wt	Lc
Dimensions [µm]	1500	600	150	5300

Figure 3: Top-Down View of Silicon Layer

Most materials were substituted in the adaptation to improve on the design. This is because some of them have drawbacks that limit performance. For instance, Macor ceramic was used because of its low thermal conductivity (1.46 $Wm^{-1o}C^{-1}$) and high operating temperature (1000 ºC). However, it has a high mass per unit length (2.52 g/cm). These changes will be enumerated in a later section.

3D PRINTING

To make material changes to this design, the avenue of 3D printing was considered. 3D printing is the creation of a physical object from a digital design, through additive manufacturing techniques[16].

The advantages of 3D printing are three-fold. The first benefit is that 3D printing allows rapid prototyping[17]. This minimises the time taken to obtain a physical model from a digital one, allowing more time to be spent on the design process. In addition to that, it works relatively well with elaborate designs. In designing a microthruster, 3D printing can allow for greater flexibility in designing intricate geometries.

The second set of benefits comes from the ability to use 3D-printed materials in the actual microthruster itself.

Additive manufacturing can be performed with certain polymers that have been used in space applications. This enables the use of these strong, lightweight polymers in the final design.

Lastly, 3D printing allows for customisability in chamber volume and, hence, in the mass of propellant carried per microthruster. This would mean that different altitude gains can be achieved, opening up the possibility of tailoring the microthrusters to specific mission objectives. This level of customisability is possible with MEMS-based technology but would incur a high fixed cost.

CHOICE OF SOLID PROPELLANT

4.1 Selection of DAATO3.5

For the new design, a solid propellant of high nitrogen content energetic molecules will be considered, namely 3,3(')-azobis(6-amino-1,2,4,5-tetrazine)-mixed N-oxides (DAATO3.5)[18]. DAATO3.5 has a high specific impulse (228 s) and a very high burn rate[19]. It decomposes at 177ºC and its density is about 1.88 g/cm^3 [20]. Upon ignition, this propellant decomposes to release mainly nitric oxide (NO) [18]. Hence, theoretical calculations involving the exhaust gas will use the properties of NO.

4.2 Pressure and Burn Rate Calculations

One can determine the pressure due to NO gas within the propellant chamber, assuming that all the solid propellant burns off immediately upon ignition, leaving only NO gas. This assumption is valid as DAATO3.5 has the highest burn rate of all known organic solids[19]. Hence, the ideal gas equation was used:

$$P = \rho RT \quad (1)$$

where P is the gas pressure, ρ is the gas density, R is the gas constant and T is the gas temperature[20]. The gas density is taken to be 1.34 kg/m^3 and the gas constant is about 0.277 kJ/kg K [21, 22]. The temperature is set at 450.15 K, the decomposition temperature of DAATO3.5. This gives a gas pressure of 167 kPa. With pressure, it is possible to determine the propellant burn rate, which follows the formula[23]:

$$Burn\ Rate = 1.69P^{0.275} \quad (2)$$

This gives a burn rate of 0.01939 m/s.

4.3 Carbonates as Proof of Concept

However, due to the explosive nature of DAATO3.5 and stringent import restrictions, a different propellant will be used in testing, to present a proof of concept.

Ammonium carbonate in its powder form was decided to be used as it possessed desirable sublimation characteristics. It decomposes at a relatively low temperature (58 ºC), releasing ammonia, carbon dioxide and water vapour, according to the equation[24]:

$$(NH_4)_2CO_3(s) \rightarrow 2NH_3(g) + CO_2(g) + H_2O(g) \quad (3)$$

HOHMANN TRANSFER ORBIT

The next step would be defining mission parameters. This was done by assuming that, in increasing altitude, the CubeSat moves from a small circular orbit to a larger one. The most fuel-efficient method of doing so is known as the Hohmann Transfer[25].

5.1 Details of the Hohmann Transfer

The Hohmann Transfer is a two-step process. Two velocity boosts, tangential to the orbits, are needed. The first pushes the satellite into an elliptical transfer orbit. Once it has completed half a period in the transfer orbit, the second boost pushes the satellite into the larger orbit. Figure 4 illustrates these orbital paths.

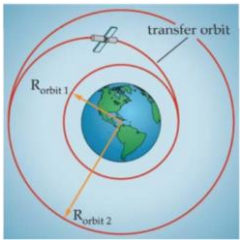

Figure 4: Orbital Paths for Hohmann Transfer[25]

5.2 Defining Mission Objectives

It is assumed that the CubeSat starts at an altitude of 350 km. Here, the thrusters will boost the CubeSat by an arbitrary value of 50 km. This altitude gain of 50 km will be the mission objective. However, it should be noted that this objective has been set as an arbitrary benchmark, and will solely be used for calculations in the design process. The ultimate aim is simply to augment orbital lifetime.

5.3 Calculations for Hohmann Transfer

From Figure 4, it can be seen that the major axis of the transfer orbit is the sum of both the smaller and larger orbital radii:

$$2a_{transfer} = R_{orbit\ 1} + R_{orbit\ 2} \quad (4)$$

The CubeSat's orbital velocity, V, can be evaluated:

$$V = \sqrt{2(\frac{\mu}{R} - \frac{\mu}{2a})} \quad (5)$$

where μ is the standard gravitational parameter. The following four parameters can be determined: $V_{orbit\ 1}$, $V_{orbit\ 2}$, $V_{transfer\ at\ orbit\ 1}$, $V_{transfer\ at\ orbit\ 2}$. These can then be used to determine the delta-V values for each boost.

$$\Delta V_n = |V_{transfer\ at\ orbit\ n} - V_{orbit\ n}| \quad (6)$$

Where n is 1 or 2. These delta-V values can be used to determine the required mass of propellant for each of the two boosts, using the Tsiolkovsky rocket equation:

$$\Delta V = I_{sp} g_o ln(\frac{m_i}{m_f}) \quad (7)$$

Where I_{sp} is specific impulse, g_o is standard gravity, m_i is the initial mass of the microthruster (with propellant) and m_f is the final mass of the microthruster (without propellant)[26]. From these equations, the first boost requires 8.453 g of propellant, while the second requires 8.384 g.

ASSEMBLING THE FIRST DESIGN

The first design was adapted from that of Chaalane et al. The aim of Design 1 was to use a working design with different materials, and test the functionality of these materials. Once it has been shown that these new materials can serve their respective purposes, a new design can be made with these materials. Only then will the above mission objectives be addressed.

6.1 Outer Shell

Chaalane's design was scaled up for easier experimentation. The propellant chamber was also enlarged to house more propellant. With this in mind, the shell around the chamber was designed and the material chosen to be ULTEM 1010. This material possessed desirable characteristics such as a high glass transition temperature (215 ºC), and no vacuum outgassing[27]. Design 1 was then 3D printed (Figure 5).

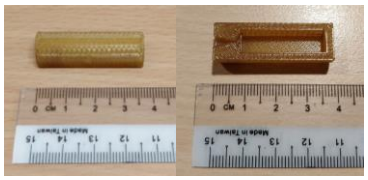

Figure 5: Design 1 Microthruster

6.2 Assembly of Design 1

The base was made of Aluminium Oxide, with a Nichrome 80/20 heating coil on the underside. This coil was connected to a power supply with copper wires.

Actual assembly was done with Loctite SI 5145. This epoxy required no mixing and cures through Room Temperature Vulcanising (RTV)[28]. It has adequate tensile strength of at least 3.4 MPa, which is sufficient for use in the proof of concept experiments. This epoxy is typically used in applications up to 200 ºC[28].

SIMULATIONS ON THE FIRST DESIGN

7.1 Stress Analysis

Stress analysis was performed using SolidWorks Simulation Xpress, for both DAATO3.5 and ammonium carbonate propellants. The aim was to determine the whether the chosen materials could withstand the high pressures in the chamber. For this analysis, it is assumed that all the solid propellant has reacted and that the pressures within the chamber are solely due to the gaseous products. This assumption holds for DAATO3.5 due to its extremely high burn rate. For the ammonium carbonate, this assumption was made to allow for a conservative analysis.

7.1.1 DAATO3.5

For DAATO3.5, the pressure due to NO gas is 167 kPa, at 450.15 K. Since all external faces of the thruster will be held in the CubeSat, a zero displacement boundary condition was imposed on the outer faces. The material properties of ULTEM 1010 were used. When data was lacking, properties of ULTEM 1000 were used instead [27 29]. Simulation results can be seen in Figure 6.

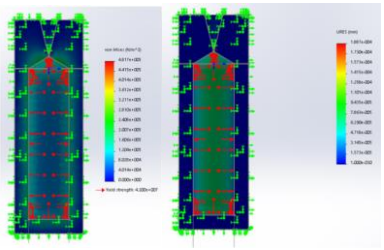

Figure 6: von Mises Stresses and Displacements of Design 1 (DAATO3.5)

At 482 kPa, the maximum von Mises stress is two orders of magnitude smaller than the material yield strength. The maximum displacement is a small $1.887x10^{-4}$ mm. Hence, ULTEM 1010 will fare well with DAATO3.5 in the first design.

7.1.2 Ammonium Carbonate

For the structural analysis with ammonium carbonate, the temperature was simulated to be 82.58 ºC, as this was the average temperature at which the experiments were conducted (see subsection 13.1). The ideal gas law (Equation 1) was applied for each gas, obtaining each of their partial pressures. These partial pressures were summed up to obtain an overall pressure of 302 kPa. With the same material properties and boundary conditions, the results can be seen in Figure 7.

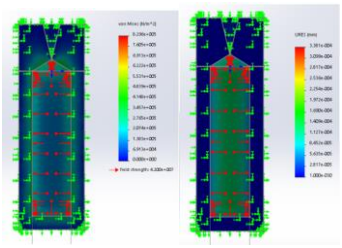

Figure 7: von Mises Stresses and Displacements of Design 1 (Ammonium Carbonate)

The maximum von Mises stress in this case is 830 kPa, which is one order of magnitude below yield strength. The maximum displacement is a negligible 3.381×10^{-4} mm. Therefore, Design 1 should have no issue with this propellant as well.

7.2 Flow Simulation

Similar to the stress analysis discussed above, a flow simulation was performed in Solidworks using Flow Simulation 2016 for both propellants. The aim of this simulation was to provide an estimate of the exit velocity of the gaseous products at the nozzle. Again, the assumption that all the solid propellant has sublimed was made. It was also assumed that the gases flowed from the back of the thruster towards the nozzle. Hence, the wall opposite to the nozzle was chosen as the inlet. An environmental pressure was 10^{-20} Pa was used.

7.2.1 DAATO3.5

The thermodynamic parameters of NO gas were used. As mentioned in subsection 4.2, the pressure of NO gas was 167 kPa, at a temperature of 450.15 K. The burn rate was 0.01939 m/s. With the inlet face area known to be 4.467×10^{-5} m^2, the volume flow rate was calculated and found to be 8.66×10^{-7} m^3/s. As the thruster will be used in LEO, the environmental temperature was set to be 394 K, which is the temperature at an altitude of 300 km[30 31]. The average exit velocity was determined to be 263 m/s.

7.2.2 Ammonium Carbonate

Another analysis was done with ammonium carbonate. As discussed in subsection 7.1.2, the pressure at 355.73 K was 302 kPa. Another input to this simulation was mass flow rate. An experiment was done to determine the sublimation rate of ammonium carbonate. For this experiment, the heating temperature was set to 85 ºC and five measurements were taken. The results are in Table 3.

Table 3: Ammonium Carbonate Sublimation Test for Mass Flow Rate

Initial Mass (g)	Final Mass (g)	Mass Change (g)	Mass Flow Rate ($x10^{-7}$ kg/s)	Heating Time (min)
1.3888	1.3171	0.0717	2.99	4
1.4154	1.2985	0.1169	4.87	
1.4075	1.2984	0.1091	4.55	
1.2963	1.2144	0.0819	3.41	
1.2979	1.1887	0.1092	4.55	

An average value of 4.07×10^{-7} kg/s was used in the simulation. The environmental temperature was set to room temperature (298.15 K) to mimic the vacuum chamber setting. The environmental pressure was kept at 10^{-20} Pa. The average exit velocity was found to be 479 m/s and the average exit pressure to be 7.89 kPa.

EXPERIMENTAL SETUP FOR THE FIRST DESIGN

8.1 Aim of Experiment

The main aim of the Design 1 experiment was to test the suitability of the selected microthruster materials. Hence, the objective is the generation of a force-time graph and the calculation of specific impulse. If these can be done, it will be concluded that the materials in Design 1 are suitable for use in a microthruster.

8.2 Experimental Setup of Equipment

A pendulum test was designed to measure displacement due to thrust. The experimental setup was inspired by a paper by Aheieva et al.[32].

The test was performed in a DUO 65-PK D46 602B Pfeiffer Vacuum chamber (Figure 8) in the Satellite Research Centre (SaRC), in the School of Electrical and Electronic Engineering (EEE), Nanyang Technological University (NTU), Singapore.

Figure 8: Vacuum Chamber in SaRC, NTU

The thrusters designed in this paper are meant to be used at an altitude of about 350 km, where the atmospheric pressure is usually between 10^{-5} and 10^{-7} mbar[33]. However, the vacuum chamber in Figure 8 was only capable of reaching a pressure of 10^{-4} mbar.

The pendulum was made using 3M Kapton polyimide tape and a nylon thread. The pendulum target was angled at 90º to ensure an inelastic collision during the experiment. Hence, the exact momentum change could be measured. Furthermore, the pendulum target will be suspended in a 60º triangle to prevent translation in other axes and to limit rotational motion (Figure 9).

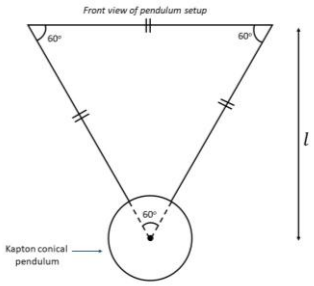

Figure 9: Front View Schematic of Pendulum Setup

By doing a balance of forces on the pendulum, the thrust can be calculated according to the equation:

$$F = Mg\frac{x}{\sqrt{L^2 - x^2}} \quad (8)$$

where x is displacement. This thrust was integrated with time to give impulse. A 'OnePlus 5T' smartphone camera was used to record the displacement of the pendulum, against a ruler, as seen in Figure 10.

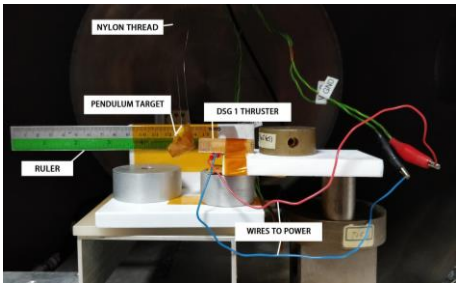

Figure 10: Actual Setup inside the Vacuum Chamber

The power consumption was standardised to 6 W for all experiments.

RESULTS AND ANALYSIS FOR DESIGN 1

9.1 Results and Analysis

For the first design, three trials were performed at a pressure of 8.60×10^{-4} mbar. For the first two trials, a laser displacement sensor was used. However, the range of the laser displacement was limited to 2 cm. Also, the placement of the sensor physically impeded the movement of the pendulum. Hence, only the third trial gave usable results. The parameters of this third trial are shown in Table 4.

Table 4: Parameters of Experiment for First Design (Trial 3)

Mass of Powder (g)	Coil Length (mm)	Pendulum Height, L (m)	Pendulum Mass (g)	Power (W)
0.371	57	0.44	0.316	6.15

Video analysis was performed and this produced the displacement-time graph in Figure 11[34].

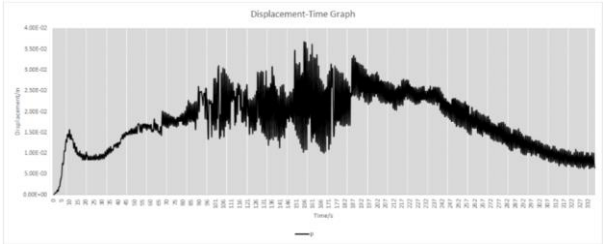

Figure 11: Displacement-Time Graph for First Design

Applying the formula mentioned in Equation 8, the force-time graph was obtained (Figure 12) and the impulse and specific impulse were calculated.

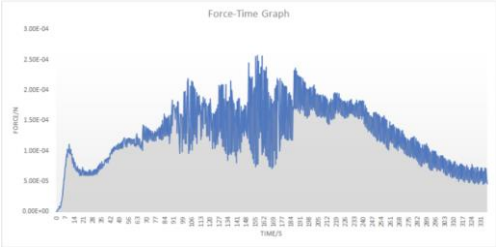

Figure 12: Force-Time Graph for First Design

$$I = 41.8\ mNs \quad (9)$$

$$I_{sp} = 11.5\ s \quad (10)$$

MOTIVATIONS FOR SECOND DESIGN

Having completed the first set of experiments with Design 1, some insight was gathered on possible improvements that could be made for Design 2. This second design will have to be made according to the defined mission objectives.

10.1 Specification of Desired Exit Velocity

As mentioned, the theoretical specific impulse of DAATO3.5 is 228 s. Specific impulse can be calculated using the following formula[35].

$$I_{sp} = \frac{1}{g_o}\left(V_{exit} + \frac{P_{exit}}{\rho V_{exit}}\right) \quad (11)$$

This formula was used to calculate the desired exit velocity, with a few assumptions. Firstly, the specific impulse was fixed at 228 s. Secondly, the exhaust pressure was taken to be approximately equal to the internal pressure in the chamber. This is validated by the flow simulation with DAATO3.5, which will be highlighted in subsection 10.3. With the values obtained from subsection 4.2, the exit velocity was calculated to be 57.2 m/s per boost.

This velocity can be achieved by means of vectorial addition of the velocities produced by 16 microthrusters, each producing a small exit velocity, of approximately 3.5 m/s. Hence, for two boosts, there will be a total of 32 microthrusters. These would be positioned as shown in Figure 13.

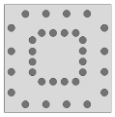

Figure 13: Approximate Positions of 32 Microthrusters

The inner 16 will be fired for the first boost, followed by the outer 16 for the second one. This ensures no torque imbalance upon firing. Hence, the key takeaway is that the nozzle design has to give an exit velocity of about 3.5 m/s per thruster.

10.2 Specification of Microthruster Volume

The first boost would use 8.45 g of DAATO3.5 propellant, and the second would use 8.38 g. With 16 microthrusters per boost, each microthruster would have to hold approximately 0.52 g of propellant. Given that DAATO3.5 has a density of 1880 kg/m^3, this would require a chamber volume of about 2.8x10^{-7} m^3 per thruster. Due to the limited volume of the CubeSat, it was decided that the 32 microthrusters should be held in a thin array. Since this is kept thin, it will only occupy a small fraction of the CubeSat.

10.3 Creation of Design 2

With the goal of achieving an exit velocity of 3.5 m/s and a chamber volume of 2.8x10^{-7} m^3 per thruster, several iterations were made and put through flow simulation. First, the goal of the exit velocity was achieved by means of altering nozzle diameter, and then the length of the chamber was adjusted to volume requirements. The optimum configuration for Design 2 was found to be a square cross-section measuring 1 cm by 1 cm, with a length of 2.8 mm, as seen in Figure 14 below.

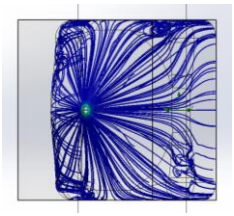

Figure 14: Flow Trajectory of Design 2 (DAATO3.5)

Design 2 above was found to produce an exit velocity of 3.731 m/s, and has a total internal volume of approximately 3.45x10^{-7} m^3, which are close to the requirements. Also, the exit pressure is 167171.12 Pa, which is very similar to the internal pressure of 167086.68 Pa, validating the earlier assumption of the exit and internal pressures being similar.

10.4 3D Printing Design 2

Design 2 was sent to be printed by the same vendor. To improve the measurability of experimental results, the entire configuration was enlarged by a factor of 3, such that the cross-sectional area measured 3 cm by 3 cm.

However, due to the nature of the ULTEM material, there was difficulty in removing the printing supports. As such, Design 2 was printed in PolyCarbonate (PC) instead. This can be seen in Figure 15. Despite PC having a lower glass transition temperature (161 ^{o}C),

than ULTEM (215 ºC), it is sufficient for use in the experiments as the first set of experiments have already proven that ULTEM works as the material of choice[36].

Figure 15: Design 2 microthruster (Enlarged)

Nevertheless, using 3D printed ULTEM 1010 on the original smaller-scaled Design 2 would still be the optimum. The support removal issue can be remedied by thickening the ULTEM layer[37]. Alternatively, the slant angle of the microthruster could be between 45º and 135º [38]. This would allow the structure to be self-supported.

However, since the Design 2 experiment is solely for measuring exhaust gas parameters, the PC shells are sufficient for use. The assembly process of the enlarged Design 2 microthruster followed that of Design 1.

SIMULATIONS ON THE SECOND DESIGN

11.1 Stress Analysis

Design 2 was also put through stress analysis. The analysis with DAATO3.5 propellant used the original Design 2, while the enlarged second design, made of PC, was used in the analysis with ammonium carbonate propellant, as this will be used in the experiment.

11.1.1 DAATO3.5

Figure 16 shows the simulation results.

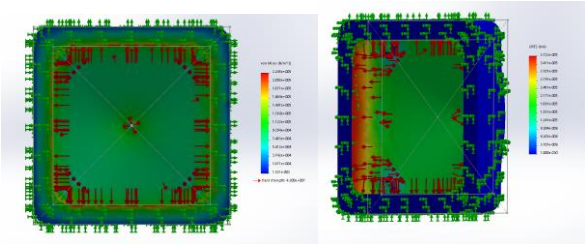

Figure 16: von Mises Stresses and Displacements on Design 2 (DAATO3.5)

The maximum von Mises stress of 0.2245 MPa is much smaller than its yield strength of 42 MPa. The maximum displacement is a negligible 3.722×10^{-5} mm. Therefore, this analysis shows that this design will work well under these loading conditions. Also, with DAATO3.5, the original Design 2 has shown large structural improvements over Design 1, as shown in Table 5.

Table 5: Structural Improvements (Design 1 to 2)

	Design 1	Design 2	Change
Maximum von Mises Stress	0.482 MPa	0.225 MPa	-53.4 %
Maximum Displacement	189 nm	37.2 nm	-80.3 %

11.1.2 Ammonium Carbonate

The stress simulation was done at a temperature of 82.58 ºC with the material properties of PC[39 40]. Figure 17 shows the results obtained.

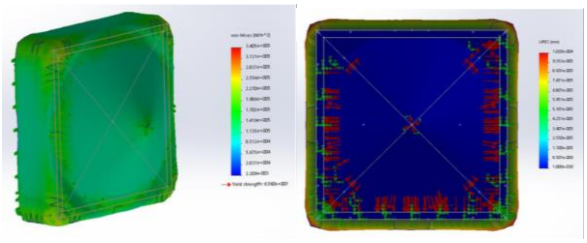

Figure 17: von Mises Stresses and Displacements for Design 2 (Carbonate)

Here, the maximum von Mises stress was 0.3405 MPa, which is two orders of magnitude lower than the yield strength of 65.6 MPa. The maximum displacement is still small, at 1.02×10^{-4} mm. These results show that structural failure will not occur when PC is used in the experiment, provided the temperature is below the glass transition temperature of 161 ºC.

11.2 Flow Simulation

11.2.1 DAATO3.5

The results of the flow simulation with DAATO3.5 have already been shown in Figure 14 earlier. To reiterate, Table 6 shows the results with DAATO3.5.

Table 6: Simulated Flow Properties of Design 2 (DAATO3.5)

Parameter	Value
Average Exit Velocity	3.731 m/s
Exit Pressure	167171.12 Pa
Specific Impulse per Thruster	2.81 s

11.2.2 Ammonium Carbonate

The simulation results for ammonium carbonate are summarised in Table 7 below.

Table 7: Simulated Flow Properties of Design 2 (Carbonate)

Parameter	Value
Average Exit Velocity	398.5 m/s
Exit Pressure	6090.75 Pa
Specific Impulse per Thruster	41.2 s

EXPERIMENTAL SETUP FOR THE SECOND DESIGN

12.1 Aim of Experiment

The aim for the Design 2 experiments is to obtain the specific impulse of the enlarged Design 2 thruster, with ammonium carbonate propellant. The pendulum displacement was plotted and translated into a force-time graph to calculate specific impulse.

This specific impulse will be compared against the specific impulse obtained from flow simulation of the enlarged Design 2 with ammonium carbonate. This will allow the derivation of an efficiency factor. This factor will then be applied to the specific impulse of Design 2 simulations with DAATO3.5, so that its actual specific impulse can be estimated.

12.2 Experimental Setup of Equipment

The experimental setup was exactly the same as that of the first design, as detailed in subsection 8.2, but with the addition of a Lascar Electronics EasyLog thermistor probe data logger (see Figure 18).

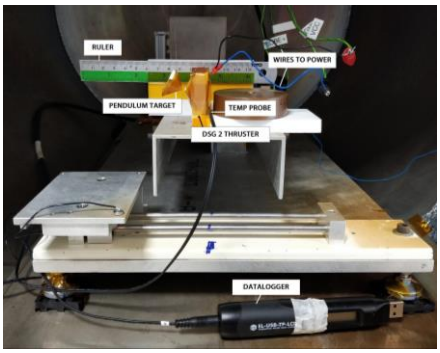

Figure 18: Experimental Setup for Design 2

Temperature data were collected twice. The probe was first placed between two parallel segments of the heating coil, and then below the coil. The supplied power was maintained at 6 W.

RESULTS AND ANALYSIS FOR DESIGN 2

13.1 Temperature Results and Analysis

The parameters for the tests are shown in Table 8 below. The pendulum mass of 0.316 g was fixed at 0.45m and the experiment had an approximate initial pressure of 9.32×10^{-4} mbar.

Table 8: Parameters of Experiment for Second Design

Trial	Mass of Powder (g)	Coil Length (mm)	Power (W)	Max Temperature of Alumina
1	2.3181	170	5.921	124.1
2	1.4346	170	6.0098	85.6

An average temperature of 82.58 ºC was obtained by obtaining the mean temperatures of each of the two experiments during the period of heating, and subsequently finding the average of these two.

13.2 Design 2 Results

Displacement results are displayed in Figure 19[35].

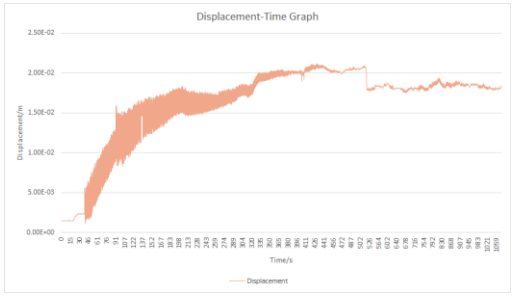

Figure 19: Displacement-Time Graph for Second Design

Applying equation (8), the force-time graph (Figure 20) was obtained and the impulse and specific impulse from the microthruster are as follows:

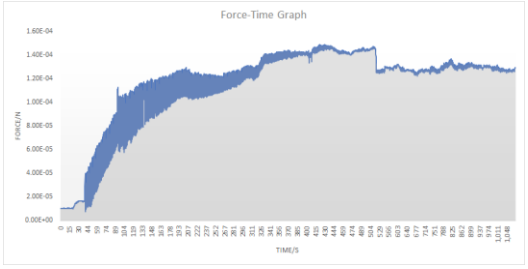

Figure 20: Force-Time Graph for Second Design

$$I = 129\ mNs \quad (12)$$

$$I_{sp} = 9.15\ s \quad (13)$$

DISCUSSION OF DESIGN 2 EXPERIMENT RESULTS

14.1 Efficiency Factor

The differences in specific impulse obtained from the simulation with ammonium carbonate and the actual experiment will be used to calculate the efficiency factor, η.

$$\eta = \frac{Actual\ Specific\ Impulse}{Simulated\ Specific\ Impulse} * 100 \qquad (14)$$

The simulated specific impulse (Table 7), was 41.2 s, and the specific impulse from experiment (Equation 13) was 9.15 s. The efficiency factor η was found to be 22.21% using Equation 14.

14.2 Application to DAATO3.5

The Design 2 simulation with DAATO3.5 gave a theoretical specific impulse value of 2.81 s per thruster (Table 6). For a set of 16 microthrusters, the total specific impulse was calculated to be 112.11 s. This was done by finding the vectorial sum of exit velocities from these 16 microthrusters and substituting this to the specific impulse formula (Equation 11).

Using η, the actual total specific impulse is therefore 24.9 s for 16 microthrusters. This would result in an altitude gain of 5.45 km. A graph was plotted using Table 1 to show the relation between altitude and orbital lifetime of a 1u CubeSat. This graph can be seen in Figure 21 below.

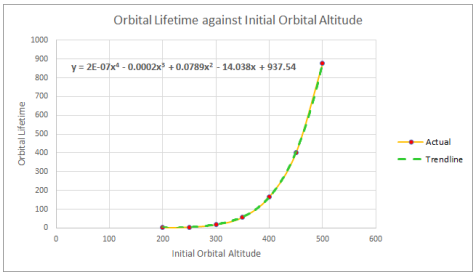

Figure 21: Orbital Lifetime against Initial Orbital Altitude

Using the trendline equation, an altitude boost from 350 km to 355.45 km will extend orbit by 11.3 days, an increase of 20%.

As mentioned in section 3, the customisability of 3D printing can be capitalized on to vary the chamber volume of Design 2, depending on mission objectives. This can be done by changing the length of the chamber, while keeping the cross-sectional area the same to keep the mass flow rate constant. Hence, depending on the mass of propellant used, different altitude gains can be achieved.

CONCLUSION

This paper has successfully achieved its aim of designing an altitude boosting microthruster. This was done by making material changes to a working design, and validating material functionality. Improvements were made and Design 2 was created to meet a mission objective. A "proof of concept" approach was adopted to predict the performance of DAATO3.5. An efficiency factor was used to determine the realisability of simulated impulse values. A 20% increase in orbital lifetime was achieved with Design 2. This can be further augmented, by using 3D printing to design a larger chamber, housing more propellant. The novelty of the 3D printing approach lies in its provision of an economical alternative to customise microthrusters. In providing a low-cost option and reducing lead time, 3D printing has addressed certain limitations of current manufacturing technologies. This potential to extend orbital lifetimes can provide the opportunity for more meaningful research with CubeSats, laying the groundwork for future space exploration.

ACKNOWLEDGEMENTS

The team would like to express our deepest gratitude to everyone who has assisted us in this project. We would first like to thank our project supervisor, Asst Prof Li King Ho, Holden, for his mentorship and guidance. We would also like to thank Dr. Chow Chee Lap, of Temasek Laboratories@NTU, for facilitating the experiments. A special thank you also goes to Peh Sheng Jue, who aided us throughout the project. We would also like to thank Mr Lim Wee Seng, Director of SaRC NTU, as well as Dr Tran Quang Vinh, a Research Fellow at the SaRC for granting us access to the vacuum chamber. Finally, we would like to thank the director of the Renaissance Engineering Programme (REP), Prof Lalit Goel, and the REP staff, for supporting this project.

REFERENCES

1. CubeSat. (n.d.). The CubeSat Program. Retrieved February 13, 2018, from http://www.cubesat.org/about/
2. Antunes, S. (2015, September 13). Your Own Satellite: 7 Things to Know Before You Go | Make:. Retrieved February 13, 2018, from https://makezine.com/2014/04/11/your-own-satellite-7-things-to-know-before-you-go/
3. Loff, S. (2017, August 4). CubeSats Overview. Retrieved February 13, 2018, from https://www.nasa.gov/mission_pages/cubesats/overview
4. Williams, M. (2017, January 06). What is Low Earth Orbit? Retrieved February 13, 2018, from https://www.universetoday.com/85322/what-is-low-earth-orbit/
5. Government of Canada, Canadian Space Agency, Directions of communications, Information services and new media. (2017, December 12). CubeSat. Retrieved February 13, 2018, from http://www.asc-csa.gc.ca/eng/satellites/cubesat/default.asp
6. Martins, J. V. (2017, January 27). Newly Created Tiny Satellites Are Key To Space Exploration. Retrieved February 13, 2018, from https://futurism.com/newly-created-tiny-satellites-are-key-to-space-exploration/
7. Qiao, L., Rizos, C., & Dempster, A. G. (n.d.). Analysis and Comparison of CubeSat Lifetime (Rep.). Sydney, NSW: Australian Centre for Space Engineering Research, School of Surveying and Geospatial Engineering, University of New South Wales. Retrieved February 13, 2018, from http://citeseerx.ist.psu.edu/viewdoc/download?doi=10.1.1.588.3019&rep=rep1&type=pdf
8. Cassady, R. J., Hoskins, W. A., Campbell, M., & Rayburn, C. (2000). A Micro Pulsed Plasma Thruster (PPT) for the "Dawgstar" Spacecraft. 2000 IEEE Aerospace Conference. Proceedings (Cat. No.00TH8484). doi:10.1109/aero.2000.878359
9. Chu, J. (2012, August 17). MIT-developed 'microthrusters' could propel small satellites. Retrieved January 08, 2018, from http://news.mit.edu/2012/microthrusters-could-propel-small-satellites-0817
10. Janson, S. W., Helvajian, H., Hansen, W. W., & Lodmell, J. (1999). Microthrusters For Nanosatellites. The Second International Conference on Integrated Micro Nanotechnology for Space Applications (MNT99). Retrieved February 13, 2018, from http://www.las.inpe.br/~jrsenna/AerospaceMEMS/Propulsao/mnt99.pdf
11. Micro Aerospace Solutions. (n.d.). Thrust Ranges. Retrieved February 13, 2018, from http://www.micro-a.net/thrusters-tmpl.html
12. Anis, A. (2012). Cold Gas Propulsion System - An Ideal Choice for Remote Sensing Small Satellites. Remote Sensing - Advanced Techniques and Platforms. doi:10.5772/37149
13. B. Larangot, V. Conedera, P. Dubreuil, T. Do Conto, C.Rossi, "Solid Propellant MicroThruster : an alternative propulsion device for nanosatellite" Aerospace Energetic Equipment Conference, Avignon, France, 2002.
14. Chaalane, A., Chemam, R., Houabes, M., Yahiaoui, R., Metatla, A., Ouari, B., Metatla, N., Mahi, D., Dkhissi, A., Esteve, D. (2015). A MEMS-based solid propellant microthruster array for space and military applications. Journal of Physics: Conference Series, 660th ser. doi:10.1088/1742-6596/660/1/012137
15. Chaalane, A., Rossi, C., & Estève, D. (2006). MEMS-based solid propellant micro -rocket with micro-igniter on thin membrane for next generation of low-cost small space and aeronautic engines (Vol. 3, Rep.). NSTI Nanotech. ISBN 0-9767985-8-1
16. 3D Hubs. (n.d.). What is 3D Printing? The definitive guide. Retrieved September 16, 2017, from https://www.3dhubs.com/what-is-3d-printing
17. "Rapid Prototyping." 3D printing solutions by Stratasys, Stratasys, www.stratasys.com/solutions/rapid-prototyping. Accessed 16 Sept. 2017.
18. Bhattacharya, A., Guo, Y. Q., & Bernstein, E. R. (2009). Unimolecular decomposition of tetrazine-N-oxide based high nitrogen content energetic materials from excited electronic states [Abstract]. The Journal of Chemical Physics, 131(19). doi:10.1063/1.3262688
19. Ali, A. N., Son, S. F., Hiskey, M. A., & Naud, D. L. (2004). Novel High Nitrogen Propellant Use in Solid Fuel Micropropulsion [Abstract]. Journal of Propulsion and Power, 20(1), 120-126. doi:10.2514/1.9238
20. National Aeronautics and Space Administration. (2015, May 5). Equation of State. Retrieved February 19, 2018, from https://www.grc.nasa.gov/www/k-12/airplane/eqstat.html
21. Air Liquide Group. (2017, April 20). Nitric oxide. Retrieved February 19, 2018, from https://encyclopedia.airliquide.com/nitric-oxide
22. The Engineering Toolbox. (n.d.). Specific Heat and Individual Gas Constant of Gases. Retrieved February 19, 2018, from https://www.engineeringtoolbox.com/specific-heat-capacity-gases-d_159.html

23. C, T. B., Son, S. F., Ali, A. N., Chavez, D. E., & Hiskey, M. A. (2005). Decomposition and Performance of New High Nitrogen Propellants and Explosives (Rep.). Sanitago, Chile: Sixth International Symposium on Special Topics in Chemical Propulsion
24. Sciencelab.com, Inc. (2013, May 21). Material Safety Data Sheet Ammonium carbonate MSDS (Rep.). Retrieved February 18, 2018, from Sciencelab.com, Inc. website: http://www.sciencelab.com/msds.php?msdsId=9927072
25. Federal Aviation Administration. (2017). Maneuvering In Space (pp. 4.1.5-191-4.1.5-221, Publication). Washington, DC: Federal Aviation Administration. Retrieved February 18, 2018, from https://www.faa.gov/about/office_org/headquarters_offices/avs/offices/aam/cami/library/online_libraries/aerospace_medicine/tutorial/media/III.4.1.5_Maneuvering_in_Space.pdf.
26. National Aeronautics and Space Administration. (2015, October 22). Ideal Rocket Equation. Retrieved February 18, 2018, from https://spaceflightsystems.grc.nasa.gov/education/rocket/rktpow.html
27. Stratasys. (2017). Ultem 1010 Data Sheet [Brochure]. Author. Retrieved February 20, 2018, from http://www.stratasys.com/materials/search/ultem1010
28. Henkel Corporation. (2014). Loctite® SI 5145™ Technical Data Sheet (Tech.).
29. GE Plastics. (2007). ULTEM* 1000 Resin (Tech.).
30. Libal, A. (2017, April 25). The Temperatures of Outer Space Around the Earth. Retrieved March 09, 2018, from https://sciencing.com/temperatures-outer-space-around-earth-20254.html
31. Estimating the Temperature of a Flat Plate in Low Earth Orbit. (n.d.). Retrieved March 09, 2018, from https://www.grc.nasa.gov/www/k-12/Numbers/Math/Mathematical_Thinking/estimating_the_temperature.htm
32. K. Aheieva, S. Fuchikami et al.,(2016) Development of a Direct Drive Vacuum Arc Thruster Passively Ignited for Nanosatellite
33. Figure 2f from: Irimia R, Gottschling M (2016) Taxonomic revision of Rochefortia Sw. (Ehretiaceae, Boraginales). Biodiversity Data Journal 4: e7720. https://doi.org/10.3897/BDJ.4.e7720. (n.d.). doi:10.3897/bdj.4.e7720.figure2f
34. Brown, D. (n.d.). Tracker (Version 4.11.0) [Computer software]. Retrieved March 18, 2018, from https://physlets.org/tracker/
35. National Aeronautics and Space Administration. (2015, May 5). Specific Impulse. Retrieved February 18, 2018, from https://www.grc.nasa.gov/www/k-12/airplane/specimp.html
36. Fortus 3D Production Systems. (2011). PC (PolyCarbonate) for Fortus 3D Production Systems [Brochure]. Author. PolyCarbonate Data Sheet
37. Bhate, D. (2016, March 1). Support Design and Removal for 3D Printed ULTEM-9085 (Case Study: Intake Manifold). Retrieved March 19, 2018, from http://www.padtinc.com/blog/additive-mfg/support-design-and-removal-for-3d-printed-ultem-9085
38. Materialise. (n.d.). Design Guidelines - Ultem 9085 - FDM. Retrieved March 19, 2018, from http://www.materialise.com/en/manufacturing/materials/ultem-9085/design-guidelines
39. Stratasys Inc. (2011). PC (polycarbonate) (Rep.). Eden Prairie, MN: Stratasys.
40. UL LLC. (n.d.). Polycarbonate (PC) Typical Properties Generic ABS PC. Retrieved March 25, 2018, from https://plastics.ulprospector.com/generics/25/c/t/polycarbonate-pc-properties-processing